Materials Research Bulletin 44 (2009) 2217–2221

Contents lists available at ScienceDirect

Materials Research Bulletin

journal homepage: www.elsevier.com/locate/matresbu

$InAs_{0.45}P_{0.55}$/InP strained multiple quantum wells intermixed by inductively coupled plasma etching

Meng Cao [a,b,*], Hui-Zhen Wu [a], Yan-Feng Lao [a], Chun-Fang Cao [a], Cheng Liu [a]

[a] State Key Laboratory of Functional Materials for Informatics, Shanghai Institute of Microsystem and Information Technology, Chinese Academy of Sciences, Shanghai 200050, China
[b] National Laboratory of Infrared Physics, Shanghai Institute of Technical Physics, Chinese Academy of Sciences, Shanghai 200083, China

ARTICLE INFO

Article history:
Received 14 January 2009
Received in revised form 8 June 2009
Accepted 2 August 2009
Available online 8 August 2009

Keywords:
A. Nanostructures
C. Atomic force microscopy
C. X-ray diffraction
D. Luminescence
D. Optical properties

ABSTRACT

The intermixing effect on $InAs_{0.45}P_{0.55}$/InP strained multiple quantum wells (SMQWs) by inductively coupled plasma (ICP) etching and rapid thermal annealing (RTA) is investigated. Experiments show that the process of ICP etching followed RTA induces the blue shift of low temperature photoluminescence (PL) peaks of QWs. With increasing etching depth, the PL intensities are firstly enhanced and then diminished. This phenomenon is attributed to the variation of surface roughness and microstructure transformation inside the QW structure during ICP processing.

1. Introduction

The quantum well intermixing (QWI) has attracted considerable interest due to its simplicity and effectivity to tune the quantum wells (QWs) properties as a post-growth method for optoelectronic and photonic integrated circuits [1,2]. By controlling the degree of QWI, the energy bandgap can be easily tailored to satisfy the requirements of different devices.

QWI can be achieved by using a variety of methods, such as ion implantation, reactive ion-etching (RIE), electron cyclotron resonance (ECR) or inductively coupled plasma (ICP) [3,4]. Recently, ICP has been exploited for high etch rate and low damage applied in a wide range of materials such as dielectrics, III–V semiconductors [5,6], etc. As exposed under the bombardment of ions in ICP, point defects are possibly generated inside the QW. Argon gas is used as it is a noble gas with relatively high atomic weight producing a high degree of intermixing. The low energy ions generated in the plasma chamber produces no direct damage to the well layers, thereby, promising no degradation of the devices photoelectric properties.

In this paper, two different $InAs_{0.45}P_{0.55}$/InP QW samples including a double-well structure with a thicker cap layer and a multiple-well structure with a thinner cap layer were used. PL enhancement phenomena on the ICP etched samples were observed. The mechanism of the PL variation can be attributed to QWI effect on the two different QWs structures, which is detailedly discussed.

2. Experiments

Two $InAs_{0.45}P_{0.55}$/InP S-QW structures were grown on InP (1 0 0) substrates by gas-source molecule-beam epitaxy (GSMBE). One structure consists of two wells with different width (from top to bottom): 3.2 and 6.6 nm with the number of 1 and 2, respectively. The barrier is 300 nm thick InP and the cap layer is 700 nm thick InP. Another structure consists of six InAsP wells with different width (from top to bottom): 2.4,3.2,4.0,5.0,6.6 and 9.6 nm, respectively, numbered from well 1 to well 6. All the barriers are 30 nm thick InP, and the cap layer is 80 nm thick InP.

Before plasma etching, half of the sample was deposited with a 420 nm thick SiN_x layer by plasma-enhancement chemical–vapor deposit (PECVD). Then the half of surface on which there is no SiN_x covered was etched to different depths by ICP. The etching gas used in ICP was Ar with a flow rate of 12 sccm. The ICP power and self-bias were 500 W and 60 V, respectively. After plasma etching, the residual SiN_x was removed by diluted HF solution. The etching depth was measured by a Talystep (XP-2) profiler. Some of the plasma etched QWs samples were annealed at 700 °C with the duration of 40 s. To avoid material decomposition, samples were covered by the InP wafer. For both of the QWs structure, all of the PL measurements were carried out at the temperature of 10 K using 514.5 nm excitation line of an Ar ion laser with a pumping

* Corresponding author at: National Laboratory of Infrared Physics, Shanghai Institute of Technical Physics, Chinese Academy of Sciences, 500 Yutian Rd, Shanghai 200083, China. Tel.: +86 21 65420850x24411; fax: +86 21 65830734.
E-mail address: mcao@mail.sitp.ac.cn (M. Cao).

0025-5408/$ – see front matter © 2009 Elsevier Ltd. All rights reserved.
doi:10.1016/j.materresbull.2009.08.006

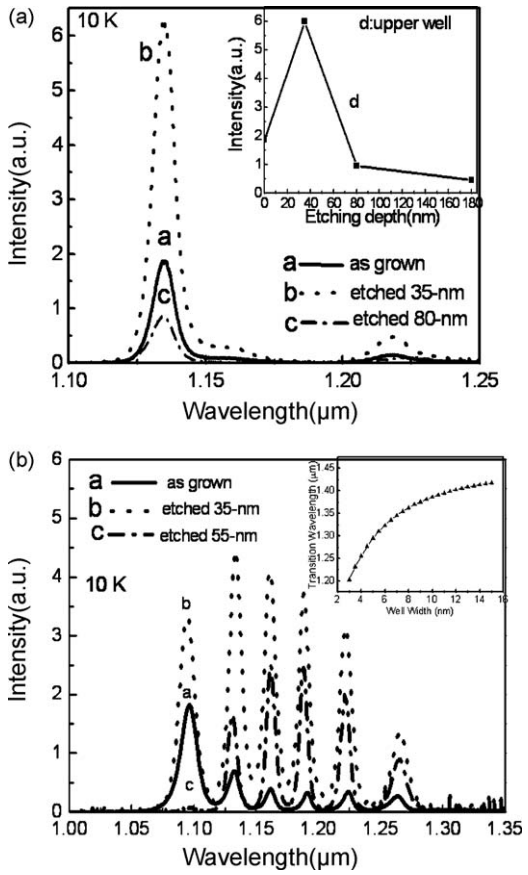

Fig. 1. 10 K PL spectra of $InAs_{0.45}P_{0.55}$/InP double QWs (a) and $InAs_{0.45}P_{0.55}$/InP MQWs (b) for different Ar ion induced etching depths. The inset of (b) shows the transition wavelength changed with well width.

power density of 13 W/cm^2 and then normalized in comparison to the intensity of the as-grown sample. Therefore their PL intensities are comparable.

3. Results and discussion

Curve a in Fig. 1(a) shows the PL spectra of the as-grown sample of $InAs_{0.45}P_{0.55}$/InP double QWs. Two PL peaks were observed which correspond to quantum transitions of the wells 1 and 2, respectively. There is an obvious little bump at the longer wavelength side of the PL peak from the upper well in the double well sample and the little bump is not reproducible from sample to sample. It is caused by the luminescence of impurities near the QW interface [7]. Curve a in Fig. 1(b) shows the PL spectra of the as-grown sample of $InAs_{0.45}P_{0.55}$/InP multiple quantum wells (MQWs). Recently, some calculations about the size and constituent stoichiometry dependence of bandgap energies in semiconductor quantum dots and wires are reported [8,9]. For QW structures, the dependence of transition wavelength (corresponding to PL peak energy or bandgap energy) on the well width at room temperature can be calculated using effective mass theory [10], as shown in the inset of Fig. 1(b). The PL peak energy will move to the higher energy with the decreasing of temperature. At low temperature 10 K, the PL peak energy changed with the composition for the InAsP bulk material can be obtained by Varshini Model [11]:

$$Eg^{InAs_xP_{1-x}} = \left(Eg_0^{InAs} - \frac{100\alpha_{InAs}}{\beta_{InAs}+10}\right)x + \left(Eg_0^{InP} - \frac{100\alpha_{InP}}{\beta_{InP}+10}\right)(1-x) + C_g x(1-x)$$

Eg_0^{InAs} and Eg_0^{InP} are InAs, InP bandgap at lattice temperature of $T = 0$ K. $\alpha_{InAs}, \beta_{InAs}, \alpha_{InP}, \beta_{InP}$ are InAs and InP temperature coefficients, respectively. C_g is the curve bowing parameter [12]. The PL peak energy of the QWs will have some blue shifts for the quantum size effect.

Curve b and c in Fig. 1(a) show the PL spectra of the plasma etched 35 and 80 nm $InAs_{0.45}P_{0.55}$/InP double QWs, respectively. The PL intensity of the ICP etched 35 nm sample is about 3.4 times that of the as-grown sample. But when the etching depth is increased to 80 nm, its PL intensity conversely decreases to less than half of that of the as-grown sample. Curve d in the inset of Fig. 1(a) shows the PL intensity of the upper well layer firstly increases and then decreases with increasing etching depth. Curve b and c in Fig. 1(b) show the PL spectra of the plasma etched 35 and 55 nm $InAs_{0.45}P_{0.55}$/InP MQWs, respectively. As shown, when the surface of the QWs is plasma etched 35 nm, its PL intensities are enhanced about 3.5 times than that of the as-grown sample when the cap layer of the QW sample is etched to 35 nm. With the etching depth increasing to 55 nm, the PL intensity of the top well almost disappears, but the PL intensities of the other well layers are still greater than that of the as-grown sample.

Under our designed parameters, the times for ICP etching to etch 35 nm InP, 55 nm InP and 80 nm InP are 25, 35 and 55 s, respectively. At the beginning, the parameters of the ICP facility need regulation to the required etching conditions and this takes about 17 s. Then, the etching rate is relative slow, and the energy of Ar ions is smaller relative to that at the first times (within 17 s). The damage to the QWs could be very small. However, the Ar ions that tunnel deeply into the QW structure significantly influence the QWs properties enhancing its PL intensities. Then, for the two MQW samples with different cap layers and barrier layers having very different thicknesses, the effects of ICP etching show similar trend for 30–50 nm etching depths. But the difference becomes significant between small etching depths (about 30 nm) and large etching depths (beyond 80 nm). This is because, with the increasing of etching depth, even though within several seconds too many Ar ions will tunnel into the quantum well and form defects that are non-radiative recombination centers that will decrease the luminescence intensity.

In fact, in our plasma-etching process, most Ar ions are stopped at a few tens of nanometers below the sample surface when the ICP power and etching depth are both small (a few tens of nanometers per min). The physical collision between Ar ions and the lattice in the cap layer generates many physical defects around the surface region. At the same time, plasma etching can lead to surface roughening. Fig. 2 shows the atomic-force microscope (AFM) images of double QWs. The root-mean-square (RMS) roughness of the as-grown and plasma etched 35 nm sample are 0.427 and 1.816 nm, respectively. Similar results were obtained from the as-grown and plasma etched MQWs. Thus the probability of photons escaping at the textured surface is increased due to angular randomization, and then the output PL intensity is enhanced [13]. We calculate the escape probability of photons from a rough surface by using the model of Yablonovitch [14]:

$$I_{esc} = 2\pi \int_0^{\theta_c} \frac{2n^2 \times I_{inc}}{2\pi} T_{esc}(\theta)\cos(\theta)\sin(\theta)\,d\theta, \quad (1)$$

$$T_{esc}(\theta) = \left(\frac{(k_z/\rho)-(k_z'/\rho')}{(k_z/\rho)+(k_z'/\rho')}\right)^2, \qquad k_z = \frac{2\pi}{\lambda}\cos(\theta), \qquad \begin{cases} TE: \rho = 1 \\ TM: \rho = \varepsilon \end{cases}$$

Here, $n\sin(\theta_c) = 1$, n is the refractive index of InP, and $T_{esc}(\theta)$ is an angle-dependent surface transmission factor. For the mirror-like

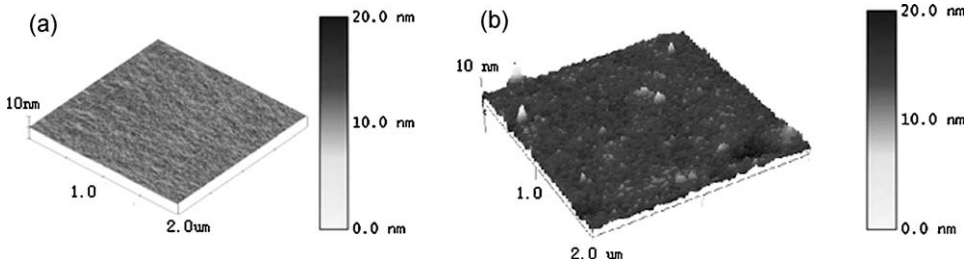

Fig. 2. AFM picture of $InAs_{0.45}P_{0.55}$/InP as-grown (a) and plasma etched 35 nm sample of double QWs (b).

(smooth) surface, the escape probability of photons is:

$$I'_{esc} = 2\int_0^{\theta_c} I_{inc}\bar{T}_{esc}\cos(\theta)\,d\theta \quad (2)$$

The calculated results show that the escape probability of photons of the plasma etched sample is only 1.6 times that of the as-grown sample. This value is obviously much smaller than the measured PL intensity enhancement (~3.5 times) of the QW samples, indicating that surface roughening is not the unique factor that contributes to the enhancement of the PL, as discussed in our previous studies [15].

In fact, even though most Ar ions are stopped at a few tens of nanometers below the sample surface, ions channeling along ⟨1 1 0⟩ is possible even at very low energies shown by molecular dynamics simulations in both silicon and III–V semiconductors [16]. Thus, a small fraction of the order ~0.1% of the incoming ions is possibly tunnelling into the materials aligned with the ⟨1 1 0⟩ axes. Then, even though the double QW samples have a cap layer that is 700 nm thick, etching only 30–50 nm will have some effects on their luminescence. On one hand, the tunnelling process of Ar ions could annihilate the grown-in defects that reside at interfaces between the barrier and well due to lattice-mismatched strain, and thus enhance the luminescence intensity [17]. The full width at half maximum (FWHM) of X-ray diffraction peaks is usually an indicator of interface uniformity and the degree of crystallinity [18]. Fig. 3 shows high-resolution X-ray diffraction (HRXRD) of the MQWs under different processing conditions. It can be seen that, for the as-grown sample (curve a), well-defined satellite peaks and interference fringes are detected up to all orders beside the (0 0 4) InP peaks indicating that the MQW structure maintains its structural integrity throughout the deposition sequence. The XRD satellite peaks appearing asymmetrically reflects that both perpendicular and lateral strain exist in our QW structure, according to kinematical theory [19,20]. Compared with the as-grown sample, the FWHM of X-ray diffraction peaks of the plasma etched 35 nm MQWs (curve b) are almost unchanged, some become even slightly smaller than that of the as-grown sample. It indicates that the tunnelling of some Ar ions annealed some interface defects inside the QW structure, which is beneficial to the sharpness of the well/barrier interface.

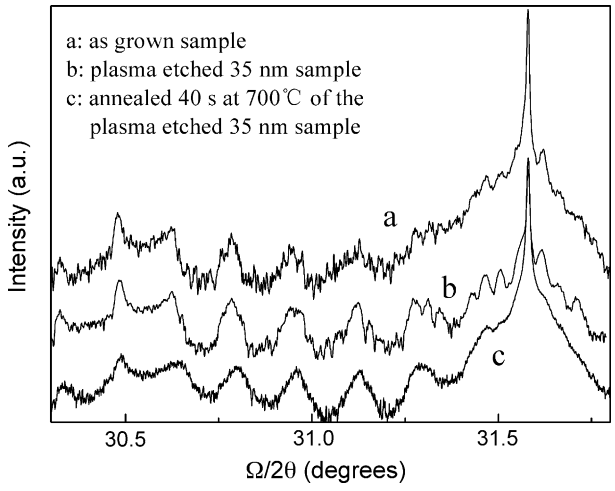

Fig. 3. (0 0 4) XRD spectra of $InAs_{0.45}P_{0.55}$/InP MQWs: (a) as-grown sample, (b) plasma etched 35-nm sample and (c) plasma etched 35 nm sample annealed for 40 s at 700 °C.

On the other hand, the difference in the electro-negativity between the Ar atom that tunnelled into the InAsP well layer and the group V atoms and the hydrostatic deformation of the lattice around the Ar sites will introduce a short-range potential, which contributes to the build-up of iso-electronic centers that can capture localized excitons [21,22]. At the same time, the tunnelling of Ar ions will introduce some In-rich region acting like quantum dots inside the QW structure [23]. Both of these processes can also increase the internal quantum efficiency. However, as shown in the inset of Fig. 1(a), the PL intensity of the upper layer of the double QWs decreases rapidly with increasing etching depth. For a large etching depth, more Ar ions will tunnel into the well layers, leading to the increase in density of Ar ions in the QWs. These accumulated high-density Ar ions form defects that are non-radiative recombination centers, and the luminescence intensity gradually decreases. With increasing etching depth, the etching surface becomes closer to the well layers and the direct bumping between Ar ions and the well layers may also lead to the deterioration of QWs PL property. Then the QWs PL intensities are decreased.

Fig. 4(a) shows PL of the double QWs measured at low temperature 10 K. An increase of PL intensities and a blue shift of peak positions have been observed in the double QWs after annealed for 40 s at 700 °C without plasma etching (curve b), which can be attributed to the thermal annihilation of grown-in defects [16]. When the cap layer of the double QWs was plasma etched 35 nm and annealed 40 s at 700 °C, its PL intensities (curve c) still increased compared with the as-grown sample (curve a). But on comparing the PL intensities change of the plasma etched 35 nm double QW sample before and after rapid thermal annealing (RTA), we found that the PL intensities of the plasma etched double QWs decreased after processing by RTA, as shown in the inset of Fig. 4(a). The decreased PL intensities of the plasma etched MWQs after processing by RTA are also shown in Fig. 4(b). The mobile point defects that were introduced into the well layers during annealing lead to the decreasing of the QWs PL intensities. It can also be seen from Fig. 4 that the PL peak positions of both the plasma etched double QWs and MQWs have an obvious blue shift at low temperature 10 K.

Point defects were generated in the cap layer as the Ar ions may knock atoms off their crystal lattice site in the sample to produce either a single isolated vacancy or a group of vacancies. During the subsequent annealing, the created point defects can effectively propagate from one lattice site to another lattice site in a random

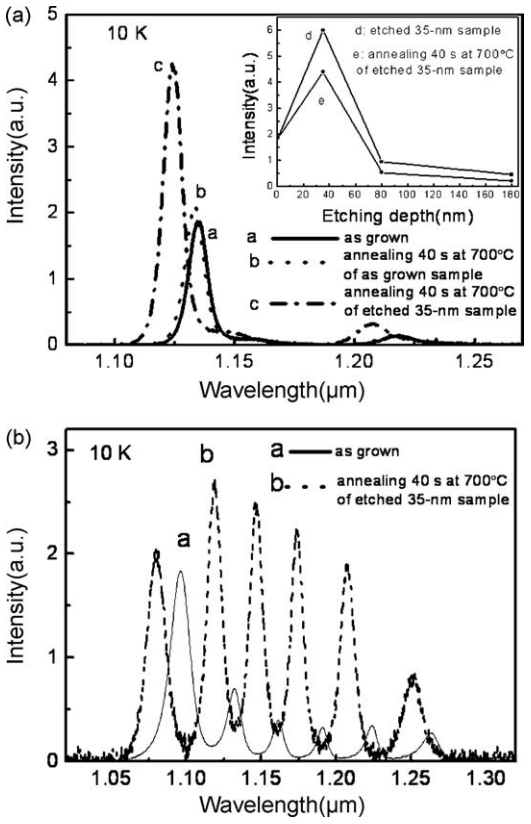

Fig. 4. 10 K PL spectra of $InAs_{0.45}P_{0.55}$/InP double QWs (a) and $InAs_{0.45}P_{0.55}$/InP MQWs (b). Curves d and e in the inset of (a) show the PL intensity of the upper well layer changed with etching depth before and after annealing, respectively.

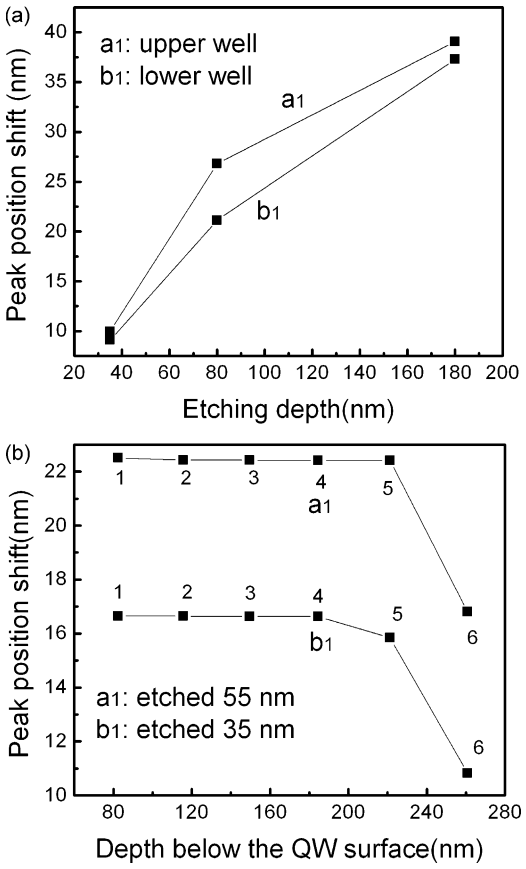

Fig. 5. Shift of PL peak positions in plasma etched $InAs_{0.45}P_{0.55}$/InP double QWs (a) and $InAs_{0.45}P_{0.55}$/InP MQWs (b) at 10 K after annealing for 40 s at 700 °C.

walk motion. The arrival of defects at the QW region enhancing the interdiffusion of the group III and group V promotes the intermixing, widens the bandgap, and results in the blue shift of PL emission [24,25].

It can be seen from Fig. 3, when the plasma etched 35 nm MQWs were processed by RTA at 700 °C, the FWHM of X-ray diffraction satellite peaks are broadened slightly compared with that of the plasma etched sample, indicating that large numbers of defects are just beginning to be introduced into the crystal and thus the interfaces of this sample become less abrupt [26]. On the other hand, no interference fringes are visible, suggesting that significant strain relaxation occurred. In fact, compositional intermixing causes the lattice distortions near the dislocated interfaces, which lead to variations in the tilting of the diffracting planes across the area irradiated by the X-ray beam causing the broadening of the satellite peaks and the loss of the thickness fringes [27,28].

The blue shift of PL peak positions for plasma etched samples under different etching conditions are compared in Fig. 5. The blue shift of the PL peak positions for the double QWs with different etching depth is shown in Fig. 5(a). The blue shift of the upper QW is 39 nm when the etching depth is 180 nm. For both well layers, the blue shift of the PL peak positions is enhanced with increasing etching depth. For the same etching depth, the blue shift of the PL peak position of the upper QW is greater than that of the lower QW, because the upper well layer is closer to the cap layer which is damaged badly and has a high density of defects. In Fig. 5(b), the depth of the different QW layers below the QW surface is clearly shown which will help us to see the PL position shift of different QW layer under the same etching depth. As shown in Fig. 5(b), the blue shift of well 1 to well 5 are of almost the same value when the etching depth is 55 nm, only well 6 has a obviously smaller value. The reason is that the barrier layer is thin (30 nm), so the quantity of the defects introduced into the well layer could be almost constant. But for the same well layer, the blue shift of the plasma etched 55 nm sample is obviously greater than that of the plasma etched 35 nm sample.

4. Conclusions

In summary, we have investigated the QWI effects on $InAs_{0.45}P_{0.55}$/InP SQWs using ICP etching and RTA. The PL intensities of QWs were firstly increased and then decreased with increasing etching depth. This is caused the variation of surface roughness and microstructure change as a result of plasma etching. The blue shift of the QWs PL positions is enhanced with increasing etching depth. For the $InAs_{0.45}P_{0.55}$/InP double quantum wells, the blue shift of the upper QW is about 39 nm when the etching depth is 180 nm. At the same etching depth, the blue shift of the PL position of the upper QW is greater than that of the lower QW due to the many more defects introduced in the upper QW.

Acknowledgement

This work was supported by the National Key Basic Research and Development Program of China under Grant No. 2003CB314903.

References

[1] O.P. Kowalski, C.J. Hamilton, Appl. Phys. Lett. 72 (1998) 581.
[2] J.E. Haysom, G.C. Aers, J. Appl. Phys. 88 (2000) 3090.
[3] J.J. He, S. Charbonneau, Appl. Phys. Lett. 69 (1996) 562.
[4] P.J. Poole, S. Charbonneau, J. Appl. Phys. 78 (1995) 2367.
[5] Djie, H.S. Mei, IEEE J. Quantum Electron. 40 (2004) 166.

[6] H. Susanto, Djie, IEEE J. Sel. Top. Quantum Electron. 11 (2005) 373.
[7] D.J. Westland, A.M. Fox, A.C. Maciel, J.F. Ryan, Appl. Phys. Lett. 50 (1987) 839.
[8] C.C. Yang, S. Li, J. Phys. Chem. C 112 (2008) 2851.
[9] Z.T. Deng, F.L. Lie, S.Y. Shen, et al. Langmuir 25 (2009) 434.
[10] Y.Q. Chen, A.Z. Li, J. Cryst. Growth 227–228 (2001) 1171.
[11] Y. Varshni, Physica 34 (1967) 149.
[12] H.P. Lei, H.Z. Wu, Y.F. Lao, et al. J. Cryst. Growth 256 (2003) 96.
[13] Y.Q. Jin, M. Lax, Phys. Rev. B 42 (1990) 9819.
[14] E. Yablonovitch, J. Opt. Soc. Am. 72 (1981) 899.
[15] M. Cao, H.Z. Wu, Y.F. Lao, et al. J. Vac. Technol. A 26 (2008) 219.
[16] K. Gartner, D. Stock, C. Wende, M. Nitschke, Nucl. Instrum. Methods Phys. Res. B 90 (1994) 124.
[17] H.S. Djie, T. Mei, J. Arokiaraj, Appl. Phys. Lett. 83 (2003) 60.
[18] C. Lamberti, S. Bordiga, J. Appl. Phys. 83 (1998) 1058.
[19] V.S. Speriosu, J. Appl. Phys. 52 (1991) 6094.
[20] P.F. Fewster, J. Philips, Research 45 (1984) 620.
[21] J.G. Zhang, X.X. Wang, Appl. Phys. Lett. 90 (2007) 081101.
[22] H.P. Gislason, B. Monemar, Phys. Rev. B 26 (1982) 827.
[23] T. Wang, D. Nakagawa, M. Lachab, Appl. Phys. Lett. 74 (1999) 3128.
[24] J. Arokiaraj, H.S. Djie, T. Mei, Appl. Surf. Sci. 237 (2004) 256.
[25] H.S. Djie, J. Arokiaraj, T. Mei, X.H. Tang, J. Vac. Technol. B 21 (2003) L1.
[26] C.A. Tran, J.T. Graham, J.L. Brebner, J. Electron. Mater. 23 (1994) 1291.
[27] R.Y.-F. Yip, A. Ait-Ouali, A. Bensaada, J. Appl. Phys. 81 (1997) 1905.
[28] P. Desjardins, M. Beaudoin, J. Appl. Phys. 80 (1996) 846.